

THE UNIVERSITY OF MICHIGAN

COLLEGE OF ENGINEERING
Department of Nuclear Engineering

Laboratory for Fluid Flow and Heat Transport Phenomena

Technical Report No. 1

ACOUSTIC NOISE FROM A CAVITATING VENTURI

Robinson
R. Garcia
F. G. Hammitt
M. J. Robinson

THE UNIVERSITY OF MICHIGAN
ENGINEERING LIBRARY

Financial Support Provided by:

NATIONAL AERONAUTICS AND SPACE ADMINISTRATION
(Grant NsG-39-60)

and

ATOMICS INTERNATIONAL
(Contract N41S6BA-002006)

administered through:

OFFICE OF RESEARCH ADMINISTRATION

ANN ARBOR

June 1, 1964

Emgn
uHK
1594

ACKNOWLEDGMENTS

Financial support for this investigation was provided by the Atomics International Division of North American Aviation, Inc., and the National Aeronautics and Space Administration.

Special thanks are also due Mr. Glenn M. Wood, Project Engineer, Pratt & Whitney (CANEL), for arranging for the processing of data on their automatic harmonic analyser; Mr. Willy Smith, graduate student in the Department of Nuclear Engineering, for his many suggestions and for the use of his tape recorder; Mr. Richard Jamron, Research Engineer, University of Michigan Willow Run Laboratories, for arranging use of the Hewlett-Packard harmonic analyser; and Messrs. Richard Ivany and David Ericson, graduate students in the Department of Nuclear Engineering, for many helpful suggestions.

ABSTRACT

A stainless steel acoustic probe for detecting cavitation incipience, degree, and intensity in a flowing fluid has been developed and tested in both mercury and water tunnel facilities at the University of Michigan. The barium titanate crystal attached to one end of the probe is used to observe the sound pattern generated by the collapsing bubbles in the venturi test section contained in each loop. The voltage generated by the crystal gives definitive information as to the degree of cavitation present. The probe is suitable for use in water-Flexiglas, mercury-Flexiglas, and high temperature liquid metal-steel systems.

It was found for both mercury and water that the signal from the probe increases as the degree of cavitation becomes more intense. For mercury the cavitation signal is proportional to the velocity raised to the 1.7 power, while in the case of water the appropriate exponent is 1.5. For mercury the cavitation signal decreased by 15% when the temperature was raised from 70 °F. to 500 °F. The frequency of the observed voltage waveforms is approximately 2 KC., somewhat higher than the frequency of the loop and pump noises present. This frequency is indicative of the frequency of the noise produced by the collapsing bubbles.

The probe is operational and can be easily and quickly installed.

TABLE OF CONTENTS

	<u>Page</u>
ACKNOWLEDGMENTS.	ii
ABSTRACT	iii
LIST OF FIGURES.	v
I. INTRODUCTION.	1
A. Importance of Detection and Measurement of Cavitation Noise.	1
B. University of Michigan Cavitation Facilities	1
C. Proposed Acoustic Studies.	1
II. RECORDING AND ANALYSIS OF AIR-BORNE NOISE	3
A. Tape Recorder System	3
B. Hewlett-Packard Harmonic Analyser.	5
C. Pratt & Whitney Automatic Harmonic Analyser.	5
III. RESULTS OF ANALYSIS OF RECORDED AIR-BORNE NOISE	5
A. Hewlett-Packard Harmonic Analyser Results, Mercury Loop.	5
B. Hewlett-Packard Harmonic Analyser Results, Water Loop	7
C. Pratt & Whitney Harmonic Analyser Results, Mercury Loop & Water Loop.	9
D. Summary and Discussion of Results.	18
IV. DESIGN OF A SUITABLE ACOUSTIC PROBE	23
A. Theoretical Aspects.	23
B. Details of Probe Design and Detecting System	24
V. ACOUSTIC PROBE DATA.	28
A. Oscilloscope Data.	28
B. Vacuum Tube Voltmeter Data	33
C. Summary and Discussion of Results.	37
VI. RECOMMENDATIONS FOR AN OPTIMUM SYSTEM	40
BIBLIOGRAPHY.	42

LIST OF FIGURES

<u>Figure</u>		<u>Page</u>
1	Cavitating Venturi Test Section.	4
2	Frequency Spectrum of Cavitation Noise in Mercury.	6
3	Frequency Spectrum of Cavitation Noise in Water.	8
4-7	Frequency Spectra of Cavitation Noise in Mercury for Various Degrees of Cavitation.	10-17
8,9	Frequency Spectra of Cavitation Noise in Water for Various Degrees of Cavitation.	19-22
10	Schematic Diagram of Acoustic Probe.	26
11	Block Diagram of Sonic Detection System.	27
2,13	Acoustic Probe Voltage Representation of Cavitation Noise From Collapsing Bubbles in Mercury	29-32
14	Effect of Cavitation Condition and Velocity on Sound Amplitude in Mercury	34
15	Effect of Cavitation Condition on Sound Amplitude in Mercury at 500 °F.	35
16	Effect of Cavitation Condition on Sound Amplitude in Mercury With Pin-Type Specimen	36
17	Effect of Cavitation Condition on Sound Amplitude in Water at 100 feet/second.	38
18	Effect of Cavitation Condition on Sound Amplitude in Water at 200 feet/second	39

ACOUSTIC NOISE FROM A CAVITATING VENTURI

I. INTRODUCTION

A. Importance of Detection and Measurement of Cavitation Noise

The use of mercury as the coolant and heat-engine working fluid in many SNAP-type reactor power plants has focused attention on the important problem of cavitation in liquid metals. At the same time cavitation is also a problem encountered in the large central station water-cooled reactor power plants, resulting in a reduced efficiency of the pump system and in some cases rendering the pump inoperable. When conducting cavitation tests in an experimental system, it is necessary to know the nature and degree of the cavitation produced under a given set of conditions. One method of determining the inception and degree of cavitation activity is to analyse the noise produced by the collapsing bubbles.

B. University of Michigan Cavitation Facilities

At the University of Michigan both mercury and water loops containing a venturi test section are available for cavitation research. These facilities have been described elsewhere.^(1,2) For low temperature tests a transparent Plexiglas venturi is suitable and, indeed, desirable in that degree of cavitation present can be visually observed. However, high temperature tests are of great interest, and such investigations require a stainless steel venturi for loop operation. Hence visual observation of the cavitation cloud is impossible, and some other means of determining cavitation inception is necessary.

C. Proposed Acoustic Studies

The technique described in this report to detect cavi-

tation incipience, degree, and intensity consists of observing the sound pattern generated by the collapsing bubbles in the venturi test section. The detection of cavitation through sonic techniques has been utilized considerably and with success in the past⁽³⁻⁸⁾. Many techniques are available, but the one chosen consisted of generating standing waves along a stainless steel rod of suitable length, one end of which was placed in close proximity to the cavitating venturi while the other end accommodated a BaTiO_3 (barium titanate) piezoelectric crystal. Collapsing bubbles generate sound waves which are propagated along the length of the stainless steel acoustic probe. The BaTiO_3 crystal is displaced slightly from its equilibrium position, and hence a small voltage is generated. This voltage is fed to an oscilloscope and a suitable high-sensitivity vacuum tube voltmeter for inspection and recording. The degree of cavitation determines the amplitude of the standing waves set up in the stainless steel probe. More severe cavitation results in greater amplitude of the sound waves and hence greater output voltage from the piezoelectric crystal. If the probe is of suitable length, it will act as a filter for sound waves of frequencies other than the resonant frequency of the rod. Hence the first step is to determine the frequency range of the sound waves generated by the collapsing bubbles and the corresponding amplitudes. This can be determined by recording directly the air-borne noise from the loop when it is operating in cavitating and non-cavitating modes. The recording must then be subjected to a harmonic analysis so as to determine an amplitude versus frequency relationship for both conditions. Comparison of the data will yield the range of frequencies

of the sound waves generated by the collapsing bubbles as the background noise due to the pump and loop are present in both cases. Then it is possible to compute the required length of a stainless steel sonic probe, so that it will be resonant in the frequency range of the sound waves generated by the collapsing bubbles. The probe is equally applicable for use in water-Flexiglas, mercury-Flexiglas, and high-temperature liquid metal-steel systems.

II. RECORDING AND ANALYSIS OF AIR-BORNE NOISE

A. Tape Recorder System

For purposes of arriving at a suitable length for the sonic probe it was necessary to first obtain some indication of the amplitude versus frequency relationship for the sound waves generated by the collapsing bubbles. In this investigation a Roberts Model 1057 four track stereo tape recorder was utilized. Tape speeds of 3 3/4 and 7 1/2 inches/sec. are possible and the frequency response shows no more than a ± 2 db. variation in the range 40-15,000 CPS. The microphone was supported in a ring stand and placed approximately 1" - 2" from the cavitating venturi. In all cases a two minute recording of air-borne noise was made. This was done for a Zero cavitation condition and for three different degrees of cavitation referred to as Visible, Standard, and First Mark. A cross-section of the venturi test section is shown in Figure 1 along with an indication of the extent of the various degrees of cavitation. Investigations were made in the mercury loop for both the Flexiglas and stainless steel venturis at velocities of 34 and 48 feet/sec. Also in the water loop studies were made for the Flexiglas venturi at velocities of 100 and 200 feet/sec. The data

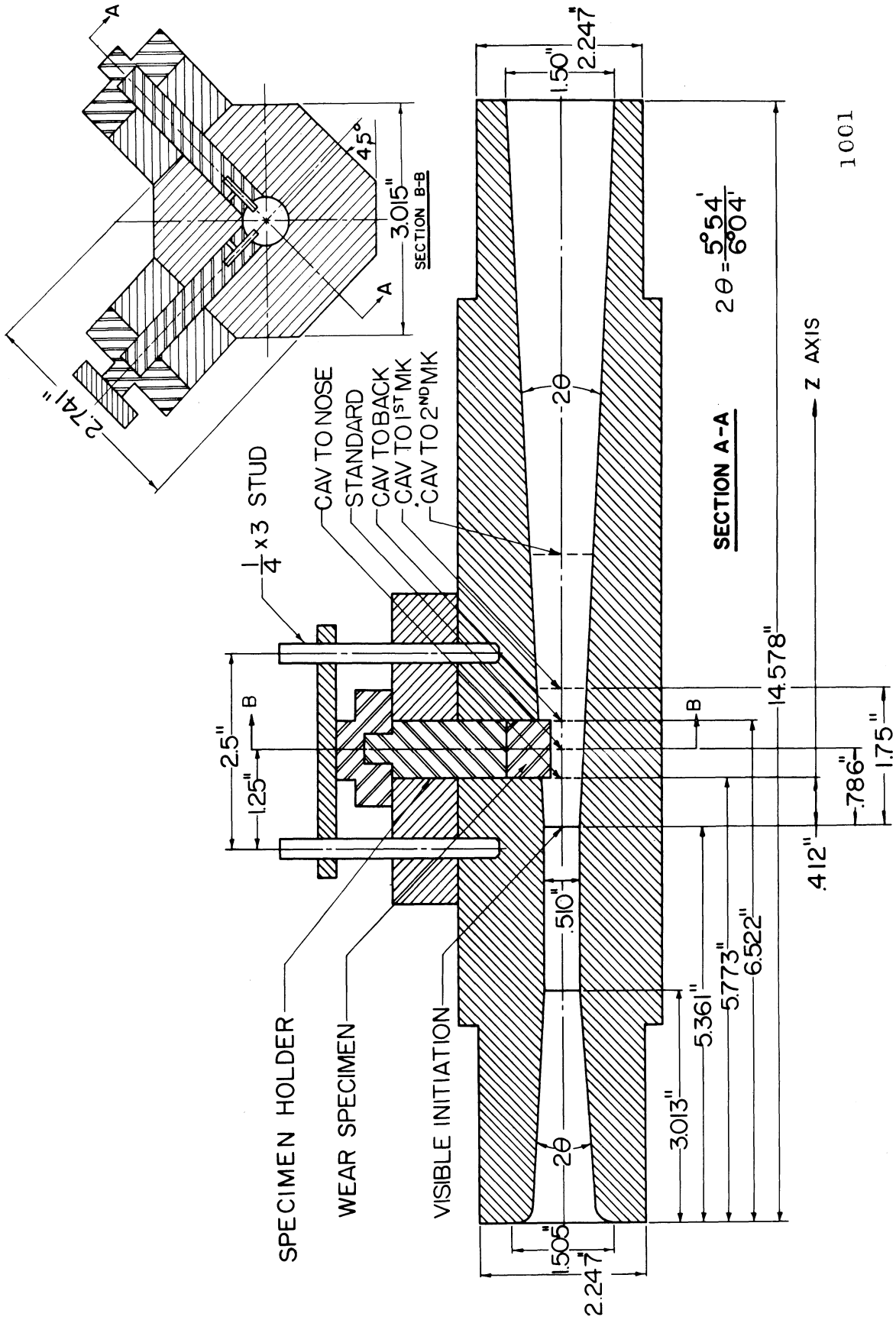


Figure 1. Cavitating Venturi Test Section

consists solely of two minute recordings of air-borne noise for the non-cavitation case and for three degrees of cavitation.

B. Hewlett-Packard Harmonic Analyser

The several recordings were subjected to a harmonic analysis to determine an amplitude versus frequency relationship. Various harmonic analysers are available for this work. The one utilized was a Hewlett-Packard Model 302A Wave Analyser having a frequency range from 50-50,000 CPS with a bandpass of 7 CPS. In analysing the tapes it was necessary to manually vary the frequency from 200 CPS to 20,000 CPS in convenient intervals and note the amplitude of the sound waves present in the narrow frequency interval. Then it is possible to compute the signal-to-noise ratio for a given degree of cavitation. The noise signal is taken to be that response obtained from recordings of air-borne noise when the loop was operating in a non-cavitating mode at the same velocity.

C. Pratt & Whitney Automatic Harmonic Analyser

The recordings were also analysed by personnel at Pratt & Whitney Aircraft (CANEL) using an automatic harmonic analyser which immediately generated plots of amplitude versus frequency for the various conditions investigated.

III. RESULTS OF ANALYSIS OF RECORDED AIR-BORNE NOISE

A. Hewlett-Packard Harmonic Analyser Results, Mercury Loop

As indicated previously recordings were made in the mercury loop for both Plexiglas and stainless steel venturis at throat velocities of 34 and 48 feet/sec. Figure 2 is a plot of Signal/Noise ratio for the mercury loop with the Plexiglas venturi

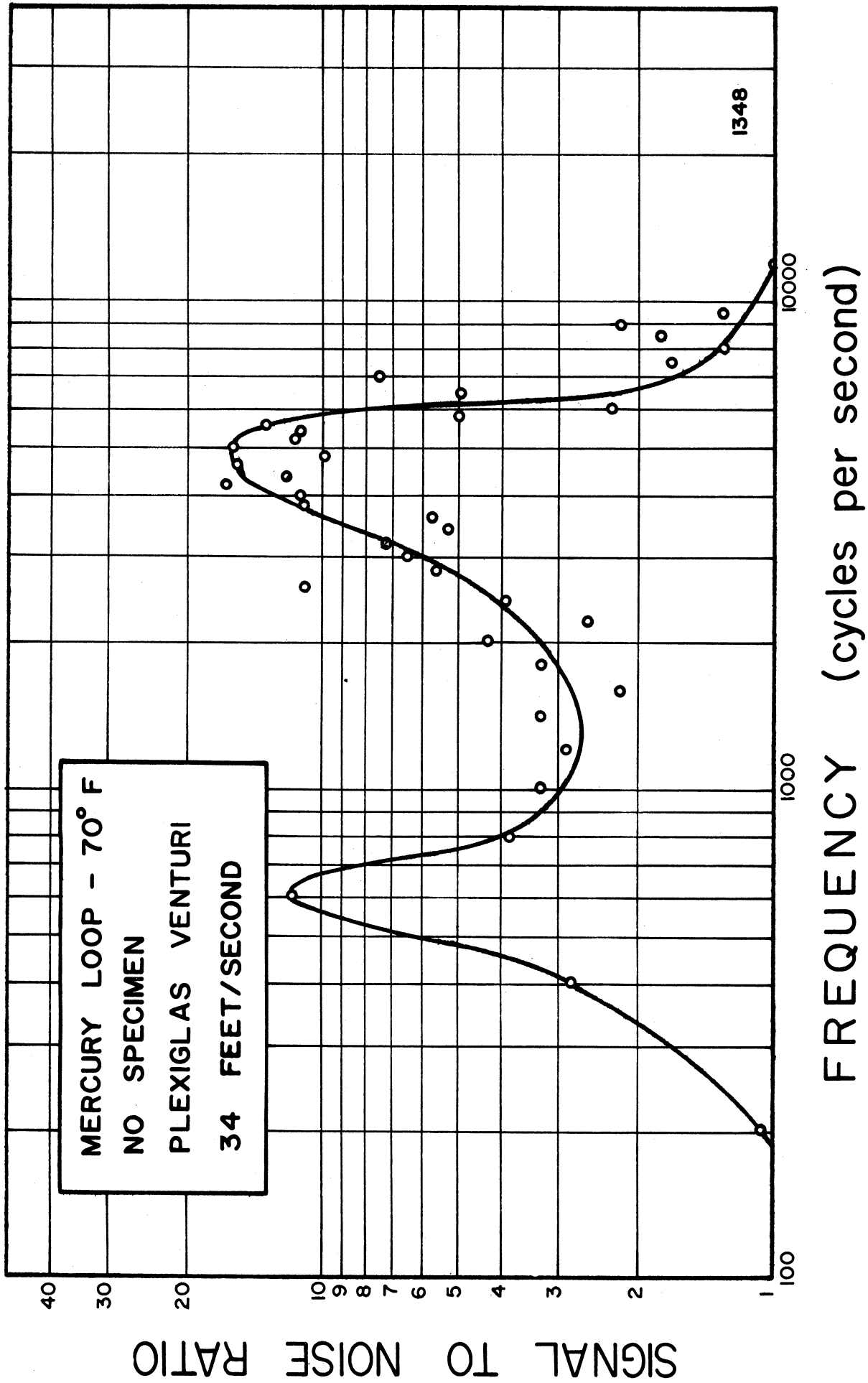


Figure 2. Frequency Spectrum of Cavitation Noise in Mercury

at a velocity of 34 feet/sec. No damage specimens were in the loop. The signal was that obtained from air-borne noise generated during First Mark (severe) cavitation. The first peak at approximately 600 CPS is possibly due to machinery vibrations excited by cavitation. The loop and pump noise is expected to be in the range 200-800 CPS, but should be present during both the non-cavitation and cavitation runs. Hence one would expect a Signal/Noise ratio of ~ 1 . The second peak at approximately 5000 CPS indicates the presence of a strong signal at this frequency during First Mark cavitation which was not present in the non-cavitating mode. This large Signal/Noise ratio definitely suggests that sound waves in the frequency range 4-6 KC are being generated by the collapsing bubbles. The data obtained at a velocity of 48 feet/sec. were not significantly different from that presented in Figure 2 for a velocity of 34 feet/sec. The data obtained with the stainless steel venturi in place with no damage specimens at velocities of 34 feet/sec. and 48 feet/sec. were inconclusive in that the Signal/Noise ratio did not differ appreciably from unity over the frequency range investigated. It is felt that this is due to absorption by the stainless steel of the sound waves generated by the collapsing bubbles. Hence only loop and machinery noise was recorded for all the runs.

B. Hewlett-Packard Harmonic Analyser Results, Water Loop

In the water tunnel facility recordings were made with a Plexiglas venturi in place at velocities of 100 feet/sec. and 200 feet/sec. with standard damage specimens in place. Figure 3 is a plot of Signal/Noise ratio for the water loop at a velocity of 200 feet/sec.

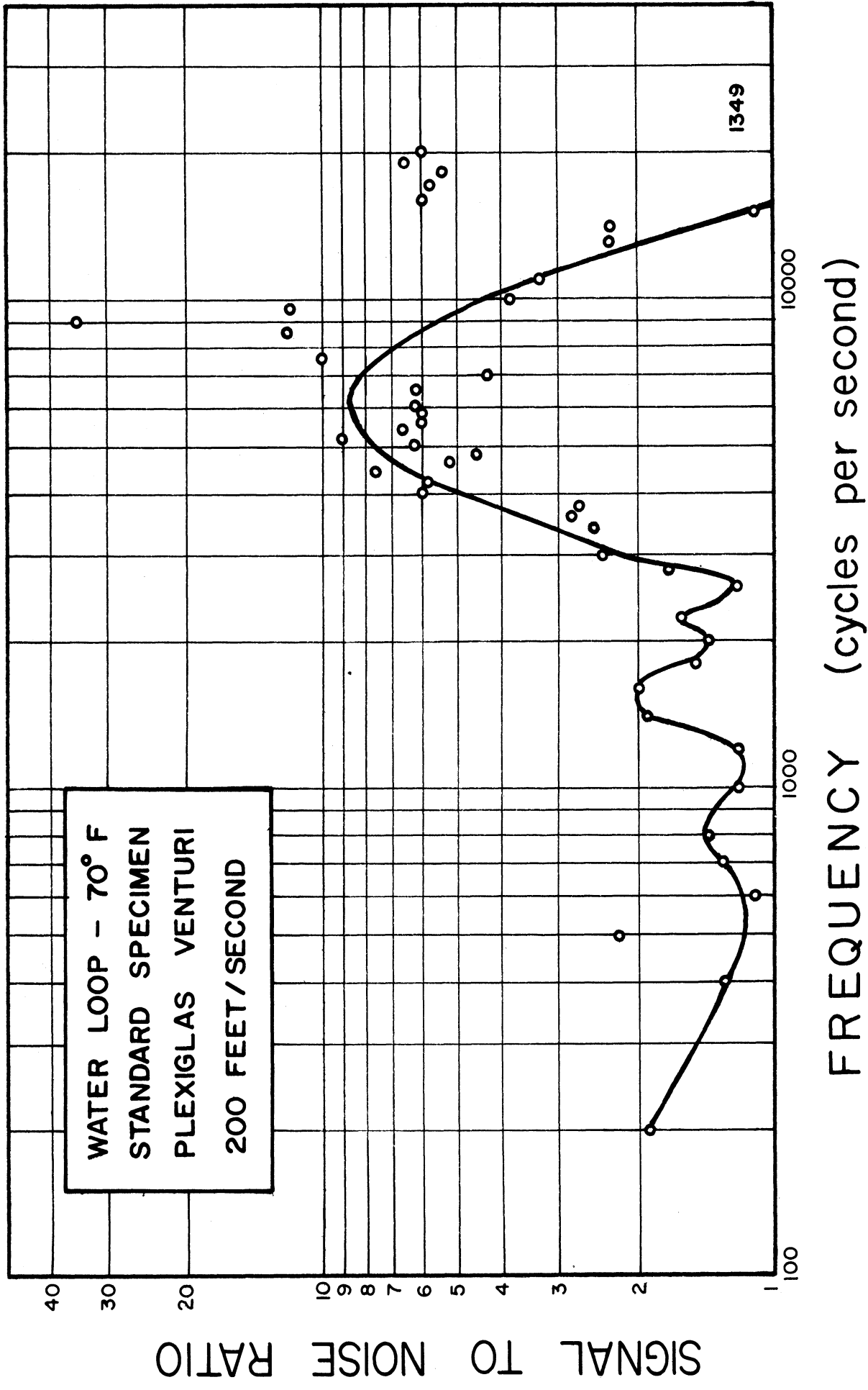
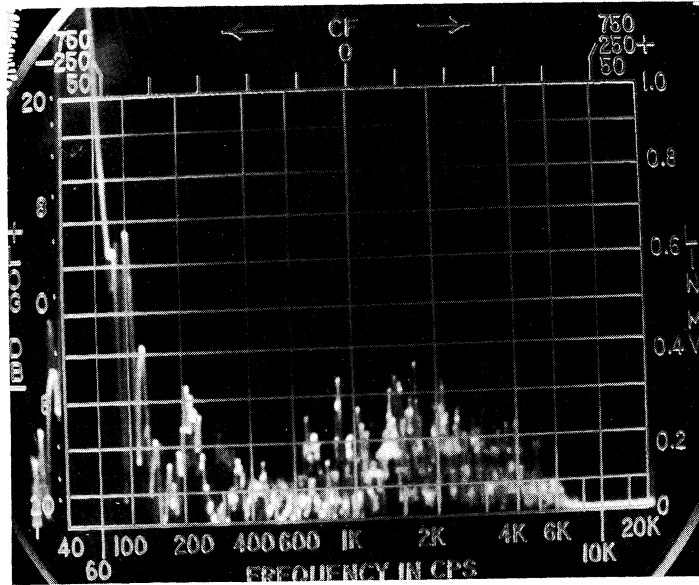


Figure 3. Frequency Spectrum of Cavitation Noise in Water

The signal was that obtained from air-borne noise generated during First Mark (severe) cavitation. Only one large peak is in evidence, and this occurs in the 4-6 KC range, similar to the peak obtained in the mercury tunnel facility. Once again one is led to the conclusion that sound waves in the frequency range 4-6 KC are being generated by the collapsing bubbles. Hence it might be concluded further that the proposed sonic probe should be made of such a length so as to be resonant in the 4-6 KC frequency range. The data obtained at a velocity of 100 feet/sec. were not significantly different from that displayed in Figure 3.

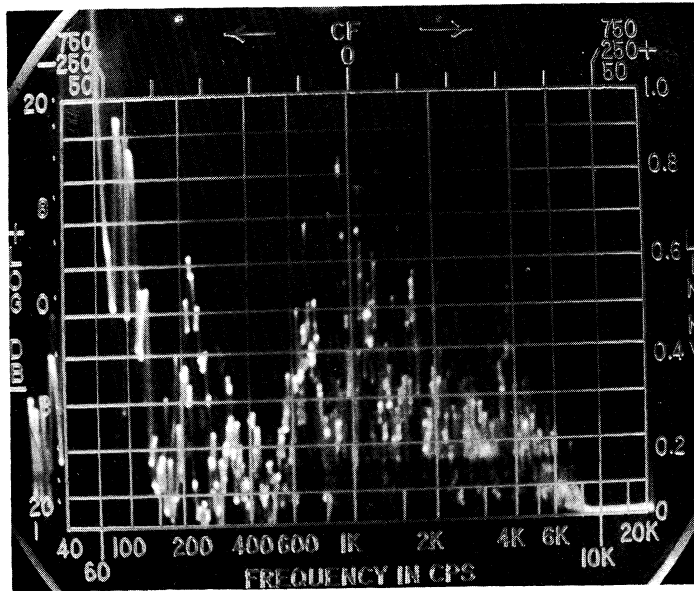
C. Pratt & Whitney Harmonic Analyser Results, Mercury Loop and Water Loop

All of the recordings of air-borne noise were also analysed utilizing an automatic harmonic analyser at Pratt & Whitney (CANEL). The output is displayed as a plot of amplitude (in db.) versus frequency. Figure 4 presents the results obtained in the mercury loop at a velocity of 34 feet/sec. with the Plexiglas venturi in place. It is clear that the signal increases in the 1-6 KC range as one proceeds from Zero cavitation to Visible cavitation, and then increases still further as the cavitation degree is increased. Figure 5 presents similar results at a velocity of 48 feet/sec. The dependence of signal on cavitation condition is clear. The effect of velocity on signal appears to be somewhat obscured as Figures 4 and 5 are quite similar. A slight increase in signal is noted at 48 feet/sec. for some sections of the spectrum, principally beyond 6 KC. The results obtained with the stainless steel venturi in place in the mercury loop at velocities of 34 feet/sec. and 48 feet/sec. are presented in Figures 6 and 7,



1350(a)

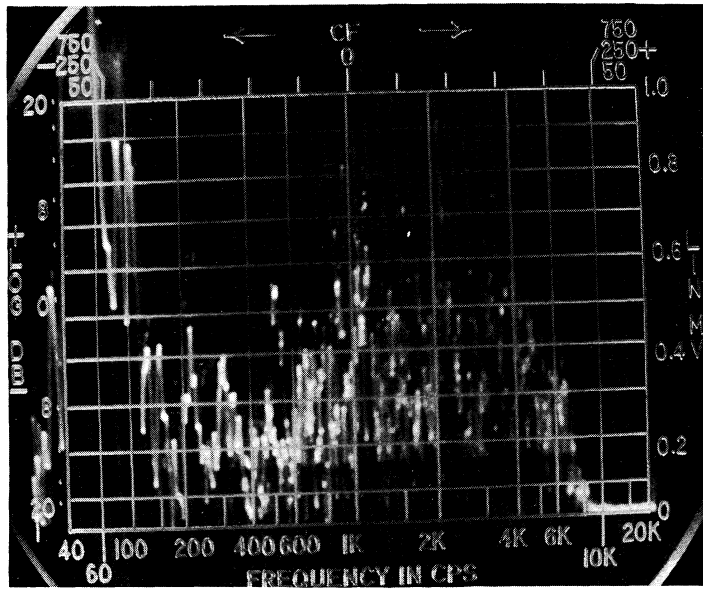
Figure 4(a). Zero Cavitation



1350(b)

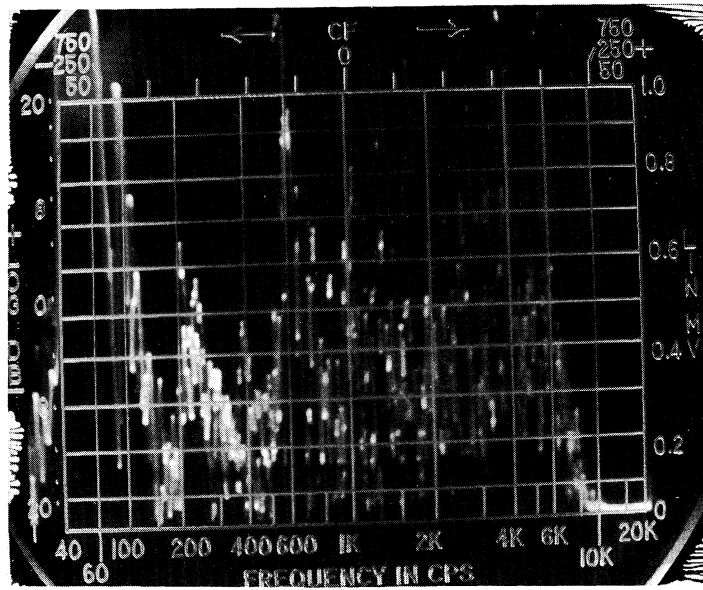
Figure 4(b). Visible Cavitation

Figure 4. Frequency Spectra of Cavitation Noise in Mercury for Various Degrees of Cavitation Plexiglas Venturi & Velocity of 34 feet/second



1350(c)

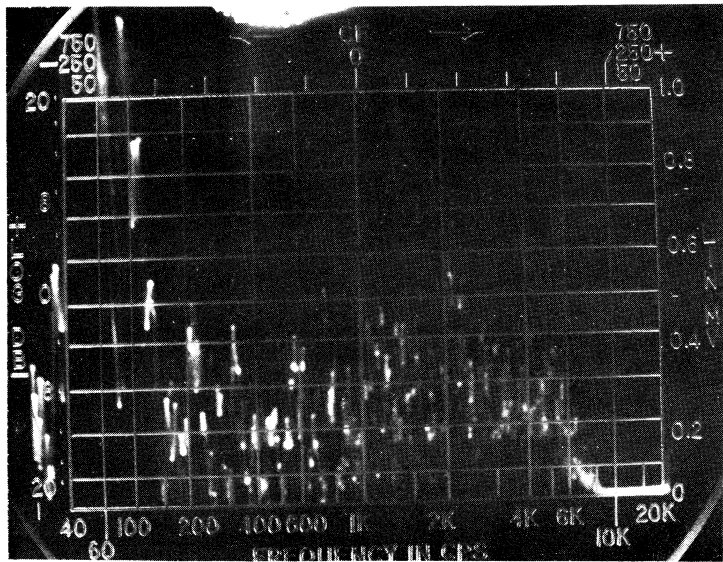
Figure 4(c). Standard Cavitation



1350(d)

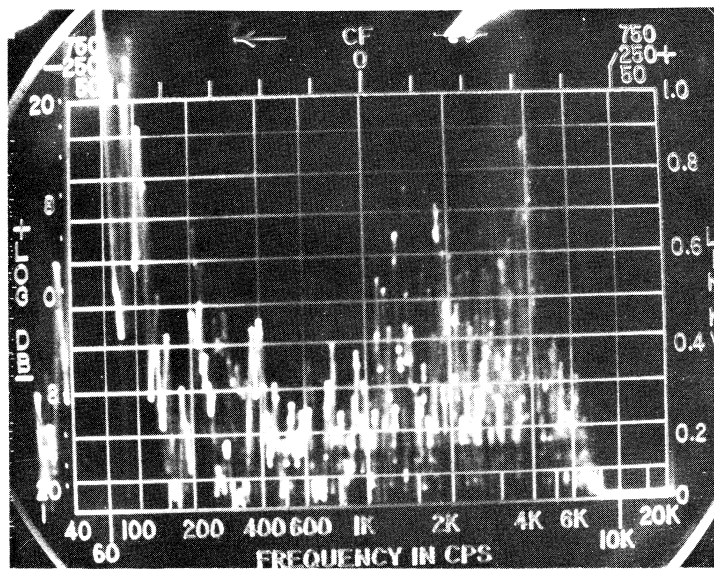
Figure 4(d). First Mark Cavitation

Figure 4 (Continued)



1351(a)

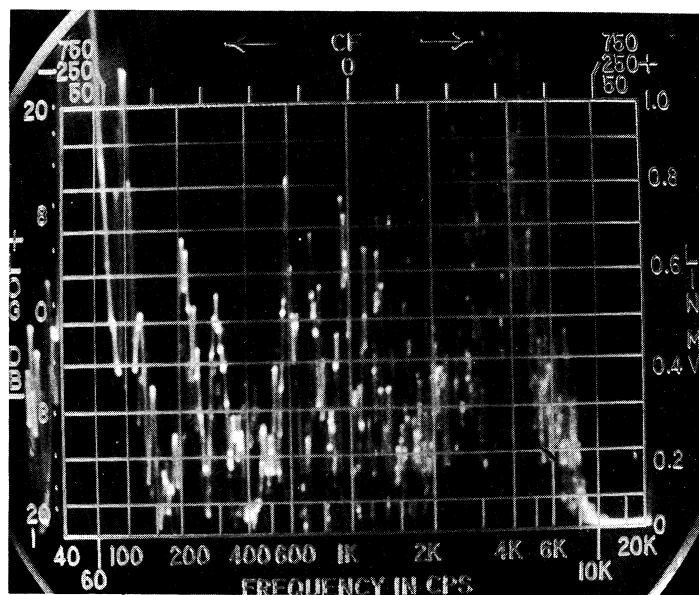
Figure 5(a). Zero Cavitation



1351(b)

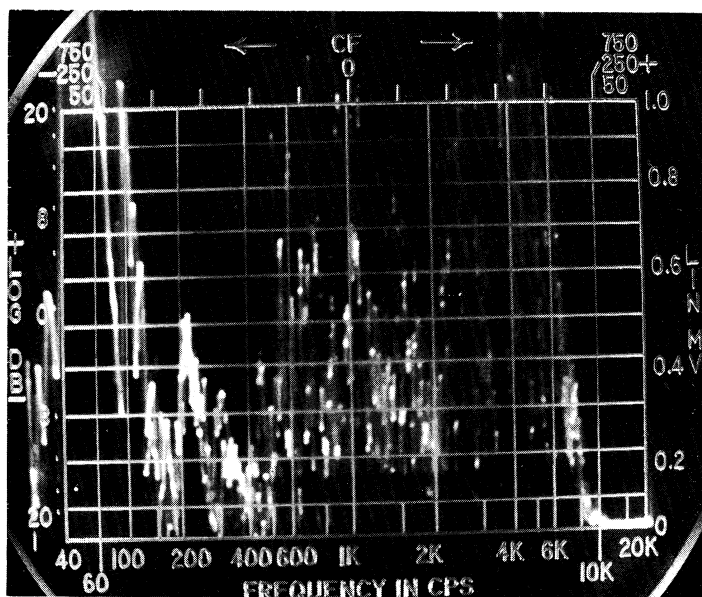
Figure 5(b). Visible Cavitation

Figure 5. Frequency Spectra of Cavitation Noise in Mercury for Various Degrees of Cavitation Plexiglas Venturi & Velocity of 48 feet/second



1351(c)

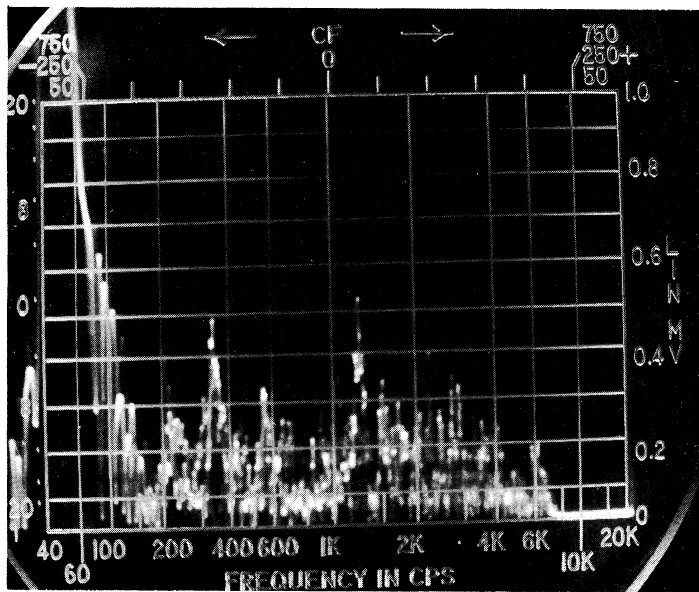
Figure 5(c). Standard Cavitation



1351(d)

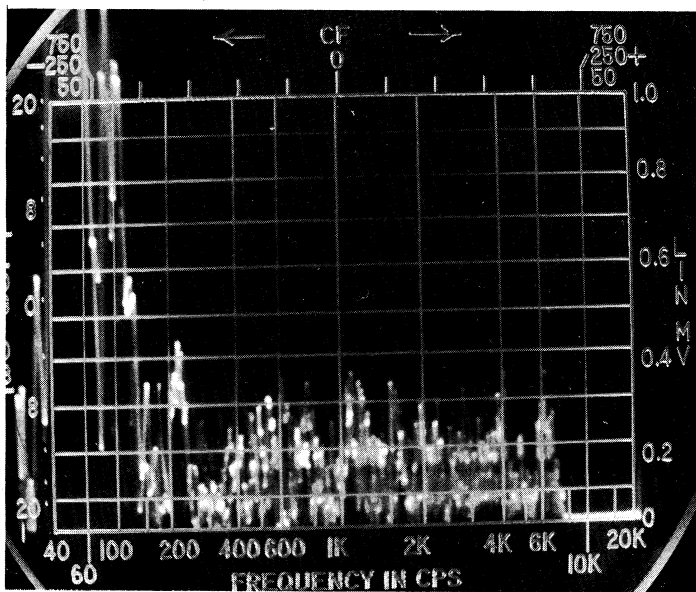
Figure 5(d). First Mark Cavitation

Figure 5 (Continued)



1352(a)

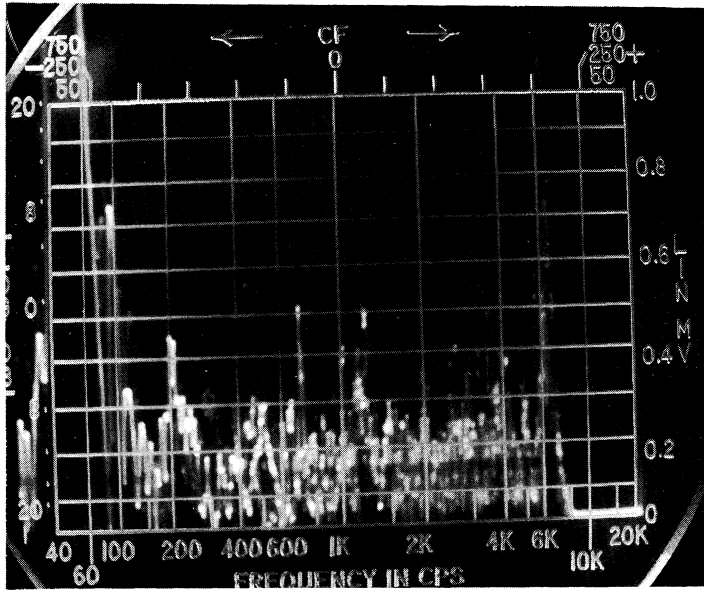
Figure 6(a). Zero Cavitation



1352(b)

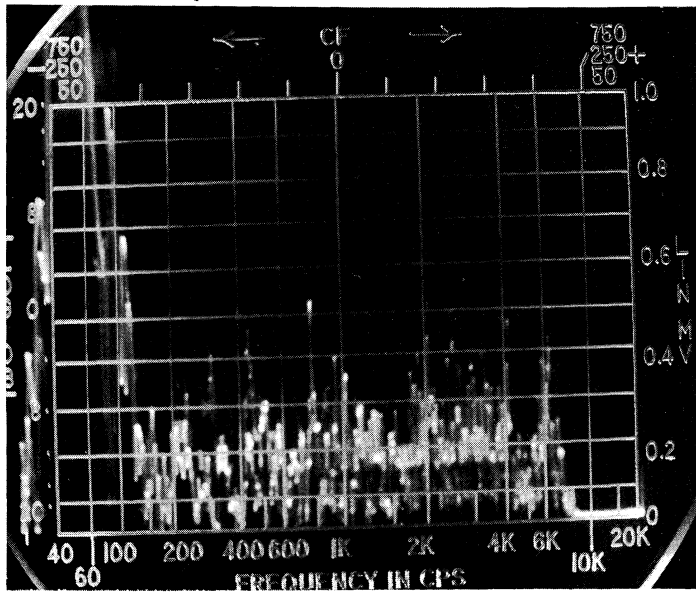
Figure 6(b). Visible Cavitation

Figure 6. Frequency Spectra of Cavitation Noise in Mercury
for Various Degrees of Cavitation
Stainless Steel Venturi & Velocity of 34 feet/second



1352(c)

Figure 6(c). Standard Cavitation



1352(d)

Figure 6(d). First Mark Cavitation

Figure 6 (Continued)

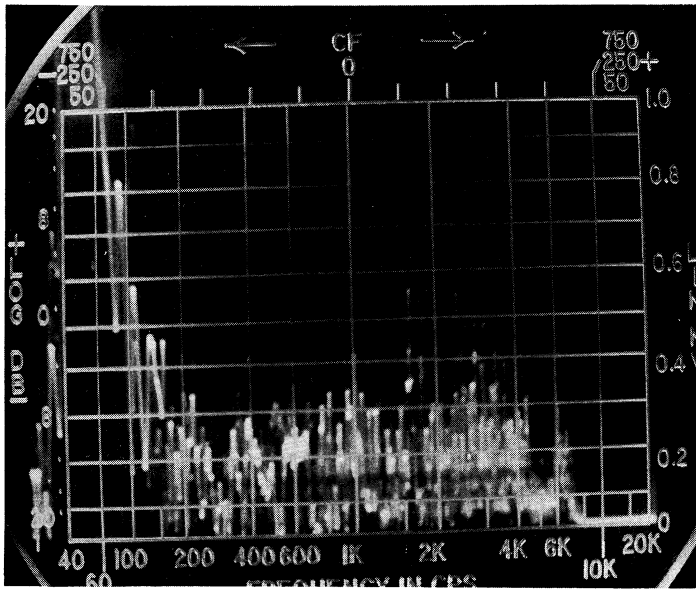


Figure 7(a). Zero Cavitation

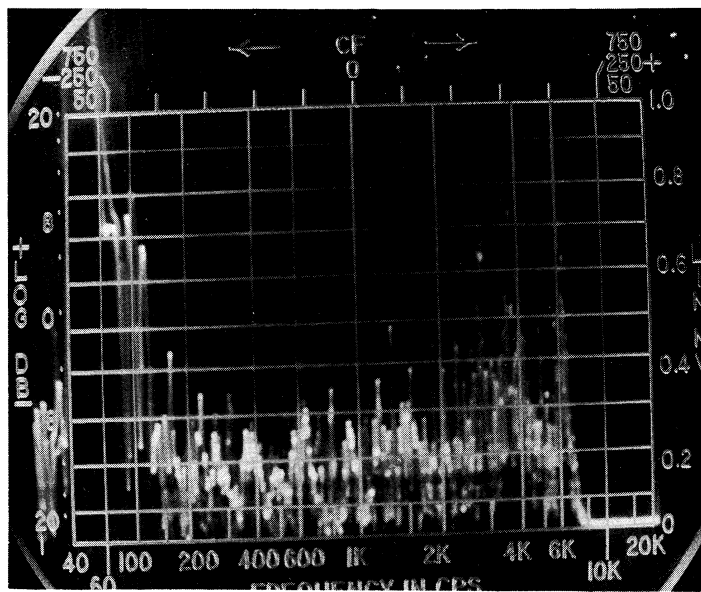


Figure 7(b). Visible Cavitation

Figure 7. Frequency Spectra of Cavitation Noise in Mercury
for Various Degrees of Cavitation
Stainless Steel Venturi & Velocity of 48 feet/second

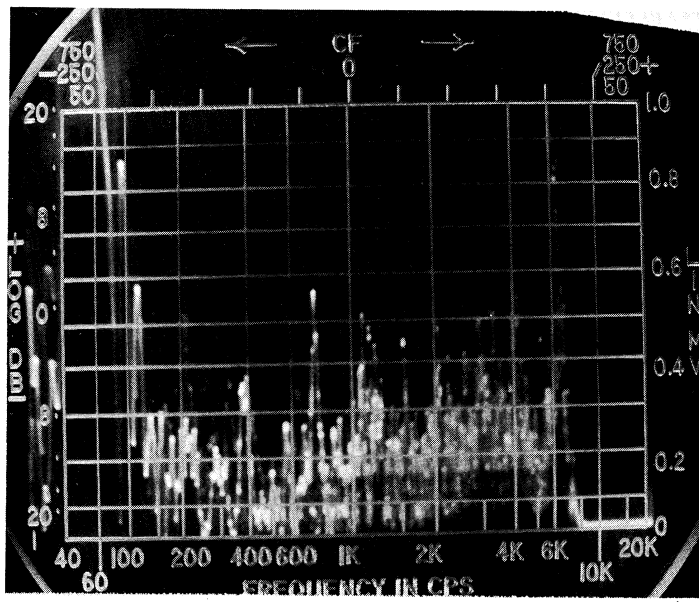


Figure 7(c). Standard Cavitation

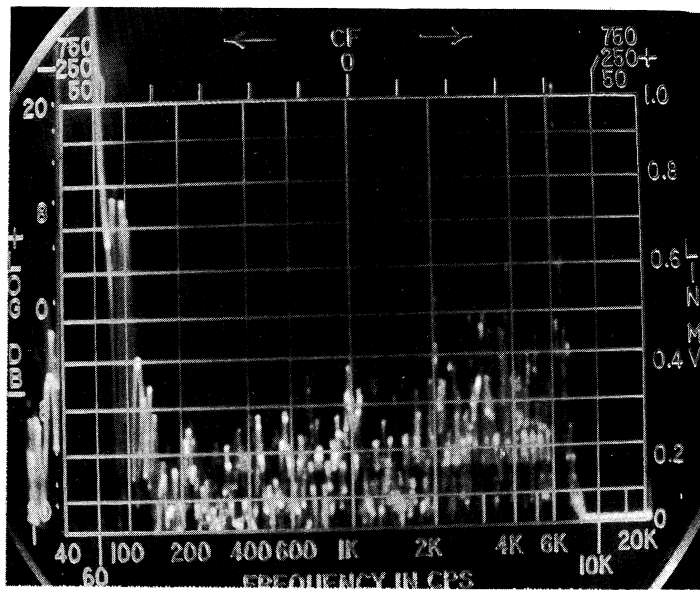


Figure 7(d). First Mark Cavitation

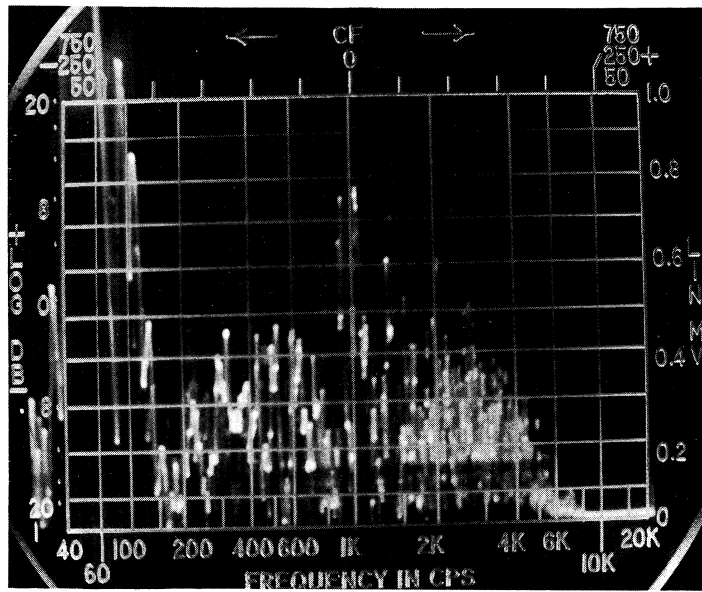
Figure 7 (Continued)

respectively. The results are inconclusive in that neither degree of cavitation nor velocity appear to significantly affect the signal obtained. Once again this is probably due to absorption of the sound waves by the stainless steel venturi. The results obtained for the water loop are presented in Figures 8 and 9. At a velocity of 200 feet/sec. the signal does not appreciably increase until Standard and First Mark cavitation are achieved. The signal at 100 feet/sec. is considerably reduced from that obtained at 200 feet/sec. for frequencies greater than 6 KC. The data from both the Hewlett-Packard harmonic analyser and the Pratt & Whitney harmonic analyser appear to be in very good agreement.

D. Summary and Discussion of Results

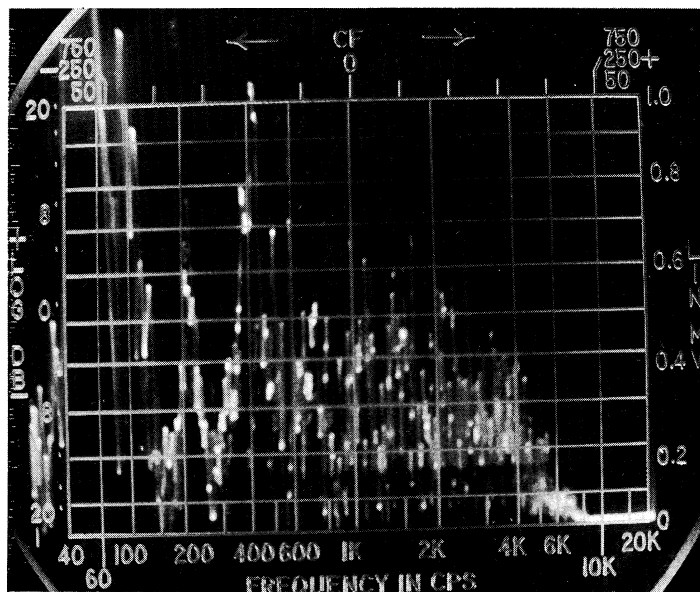
The following statements summarize the results of the air-borne noise study:

1. For either mercury or water the signal increases with increasing velocity for frequencies above 6 KC. In the case of mercury this is true for both the Plexiglas and stainless steel venturis.
2. The mercury and water spectra are very similar in form. The signal does not appear to be a strong function of the test fluid.
3. In the case of mercury the signal appears to be considerably attenuated when the stainless steel venturi is in place. Apparently the sound waves are absorbed more completely in the stainless steel than in the Plexiglas. As a result, the Signal/Noise ratio is \sim unity with the stainless steel venturi in place.



1354(a)

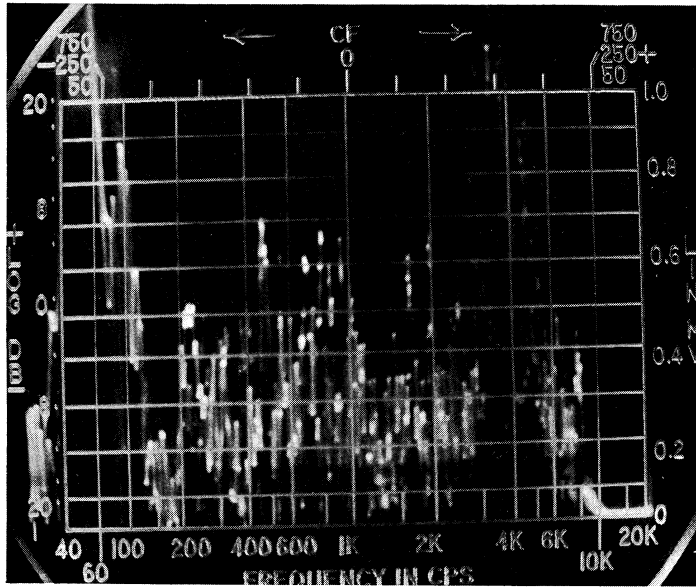
Figure 8(a). Zero Cavitation



1354(b)

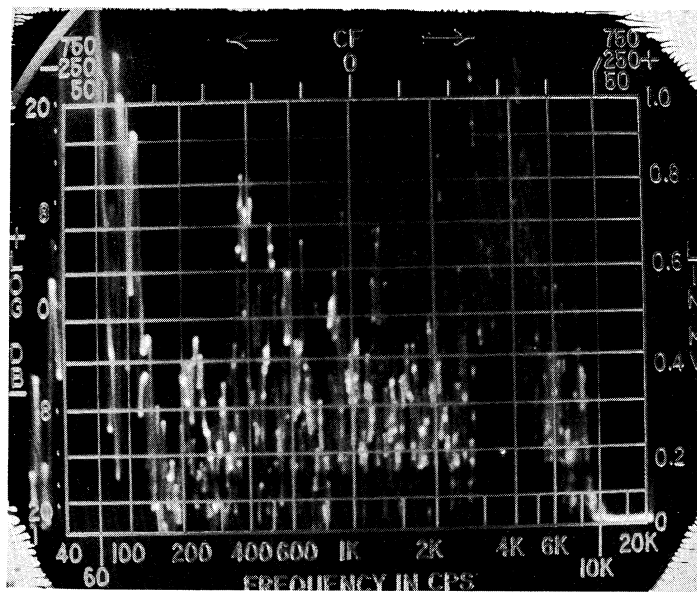
Figure 8(b). Visible Cavitation

Figure 8. Frequency Spectra of Cavitation Noise in Water for Various Degrees of Cavitation Plexiglas Venturi & Velocity of 200 feet/second



1354(c)

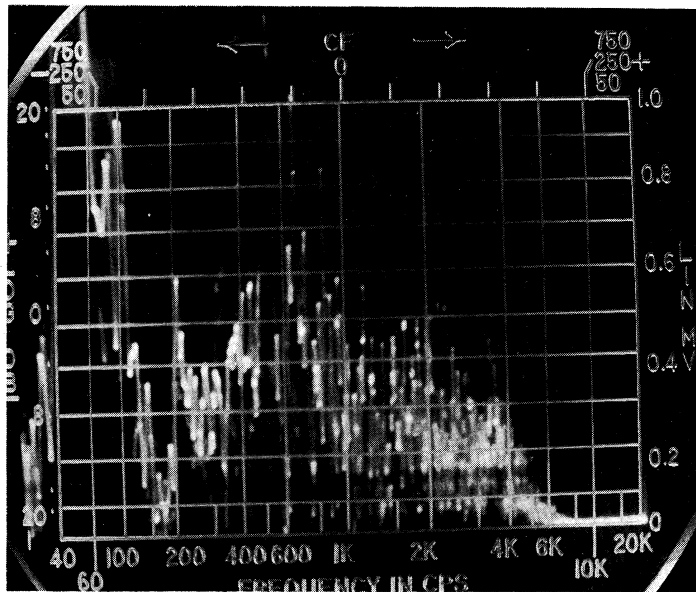
Figure 8(c). Standard Cavitation



1354(d)

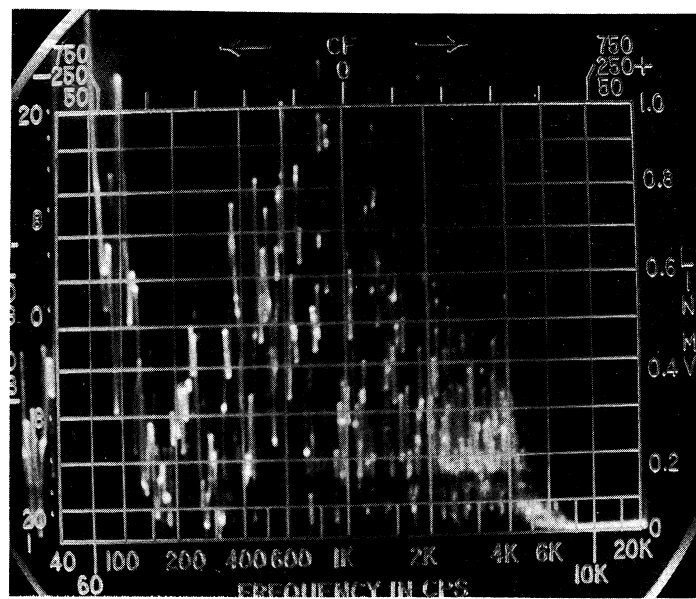
Figure 8(d). First Mark Cavitation

Figure 8 (Continued)



1355(a)

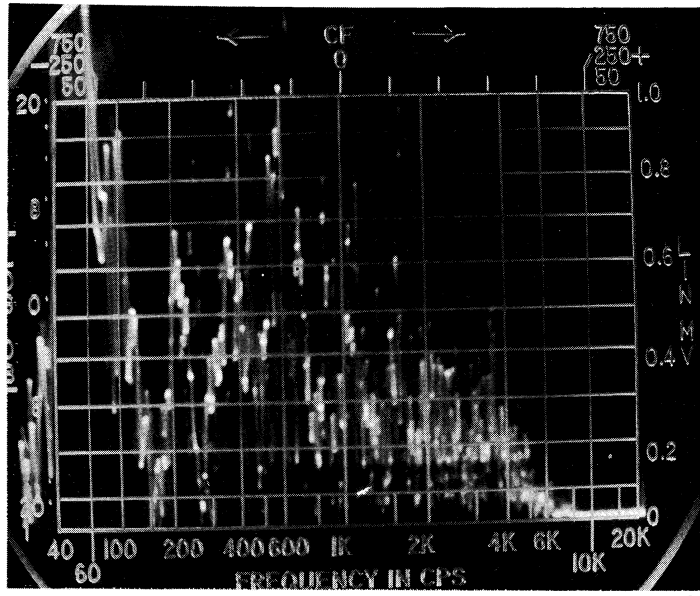
Figure 9(a). Zero Cavitation



1355(b)

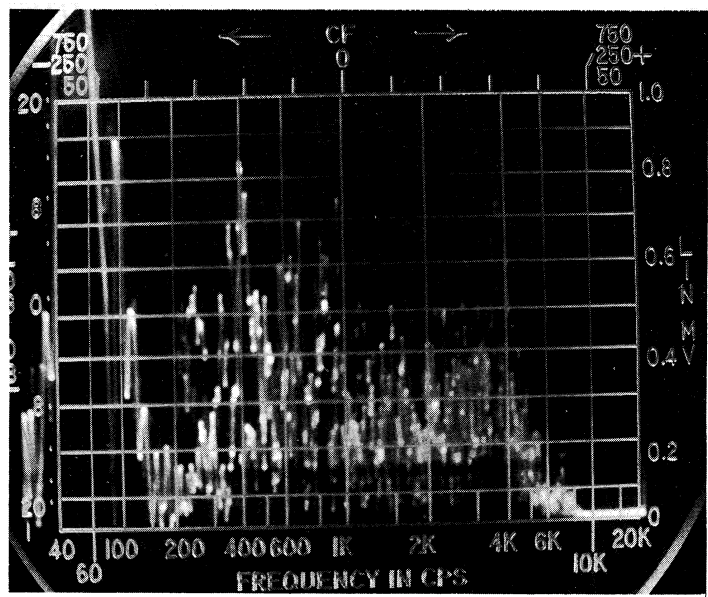
Figure 9(b). Visible Cavitation

Figure 9. Frequency Spectra of Cavitation Noise in Water for Various Degrees of Cavitation Plexiglas Venturi & Velocity of 100 feet/second



1355(c)

Figure 9(c). Standard Cavitation



1355(d)

Figure 9(d). First Mark Cavitation

Figure 9 (Continued)

4. For both mercury and water the signal increases as the degree of cavitation becomes more intense. In the case of mercury this is true for both the Plexiglas and stainless steel ventururis.

5. All signal seems to end at about 8-9 KC in Figures 4-9. This apparently is due to frequency cut-off of the Pratt & Whitney harmonic analyser since a signal was obtained beyond 8-9 KC when the Hewlett-Packard harmonic analyser was used.

6. Considerable high frequency signal is noted for the case of Zero cavitation in water especially at a velocity of 200 feet/sec. This may indicate presence of cavitation on an invisible scale.

7. Generally for either fluid cavitation noise is approximately "white" from about 200-6000 CPS (at least).

8. Since the Signal/Noise ratio is maximum in the 4-6 KC frequency range for both mercury and water, the length of the proposed sonic probe should be such as to make it resonant in this frequency range.

IV. DESIGN OF A SUITABLE ACOUSTIC PROBE

A. Theoretical Aspects

It is desired to generate standing waves along the length of a stainless steel rod, which is fixed at one end and whose other end is free. According to Den Hartog⁽⁹⁾ the resonant frequency of a cantilever which is set in longitudinal vibration is given by:

$$f_n = \frac{(n+1/2)}{2} \sqrt{\frac{AE}{\mu_p L^2}}$$

where:

A = cross-sectional area of cantilever

E = modulus of elasticity of material

μ_1 = mass per unit length of rod

L = length of rod

n = 0, 1, 2, 3, ---- = number of nodes.

In the case of stainless steel the expression becomes:

$$f_n = (2n + 1) \frac{51,000}{L} \quad \begin{array}{l} f_n \text{ in CPS} \\ L \text{ in inches} \end{array}$$

For n = 0, we have:

$$f = \frac{51,000}{L}$$

Choosing a value of 5000 CPS for f, we have:

$$L = \frac{51,000}{5,000} \approx 10''$$

Hence it appears that the proper length of the probe should be approximately 10". Two probes were fabricated, one of length 10" and the other of length 24". In the ensuing measurements it appeared that the signal obtained with the 24" probe was maximum. Hence it was adopted as the standard length. This discrepancy in length calculation is unexplained at this time.

B. Details of Probe Design and Detecting System

As mentioned previously it is desired to detect cavitation incipience, degree, and intensity by means of observing the sound pattern generated by the collapsing bubbles in the venturi test section. This can be done by generating standing waves along a stainless steel rod of suitable length, one end of which is placed in close proximity to the cavitating venturi while the other end accommodates a suitable piezoelectric crystal. Piezoelectric crystals

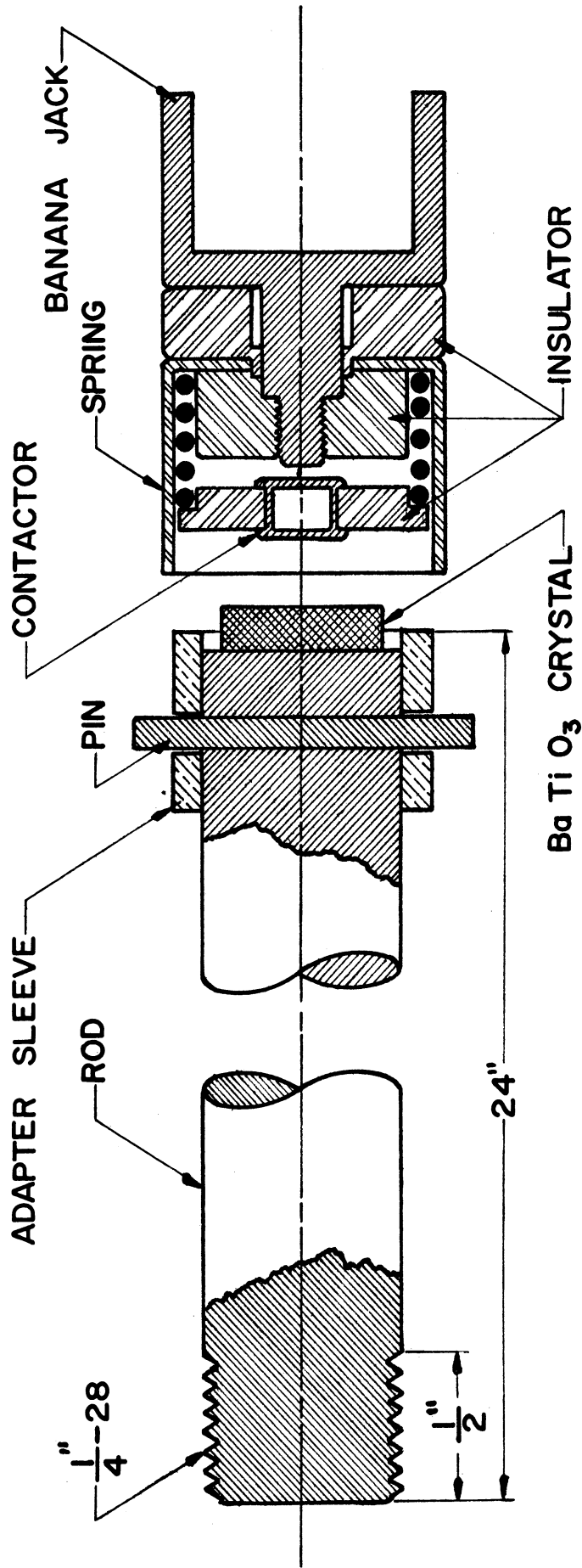
of adequate sensitivity are highly temperature-sensitive and cannot be used above rather moderate temperatures. Also the design should be applicable to all fluids to be tested. It seems evident that an arrangement suitable for high-temperature liquid metals must isolate the crystal sufficiently from the system to allow the maintenance of low temperature. Also, the probe should not penetrate the venturi wall because of possible sealing problems. Hence the following are the major features of the sonic probe design:

1. A stainless steel rod of circular cross section having a diameter of $1/4$ " and a length of 24 " was adopted as a standard.

2. $BaTiO_3$ was selected as the piezoelectric crystal despite its severe temperature limitation (200 °F.) because of its high sensitivity. The crystal is $3/16$ " diameter by $.02$ " thick and was cemented to one end of the stainless steel rod. One side of the crystal was grounded directly to the stainless steel rod; the other side was connected to a modified banana jack which was spring-loaded against the crystal. This arrangement makes it simple to monitor the output from the crystal with either a cathode-ray oscilloscope or suitable low-level vacuum tube voltmeter. The probe must be shielded to minimize 60-cycle pick-up which can be a problem.

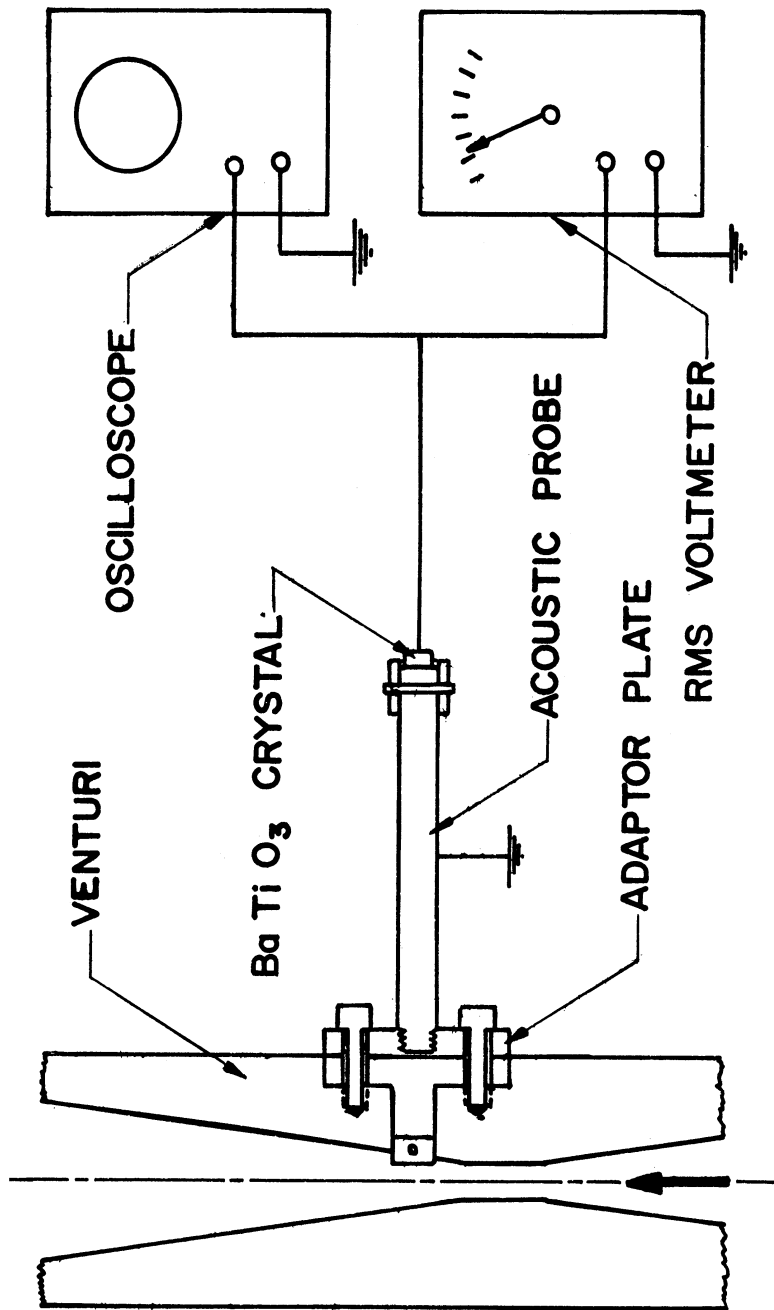
3. The other end of the rod was fitted with a $1/4$ " - 28 thread. This made it possible to screw the probe into any one of several venturis, each of which had been fitted with an adapter plate.

The details of the probe design are shown in Figure 10. Figure 11 is a schematic diagram of the sonic probe and the detecting system. The signal from the crystal can be monitored either with the oscilloscope or the vacuum tube voltmeter.



1356

Figure 10. Schematic Diagram of Acoustic Probe



1357

Figure 11. Block Diagram of Sonic Detection System

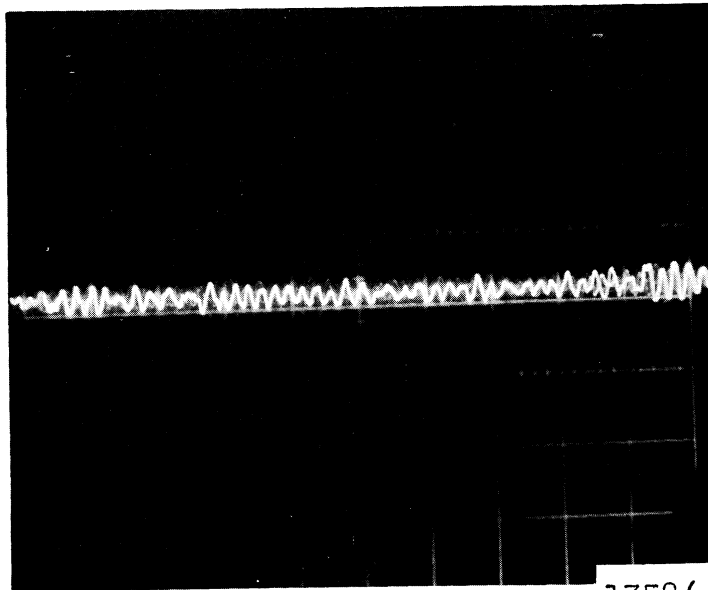
It was found that the output from the crystal generally varied from 0-50 mv. Hence a sensitive low-level vacuum tube voltmeter was needed. A Ballantine Model 300-D vacuum tube voltmeter with a voltage range of 1 mv - 1000 V, a relatively flat frequency response from 20 CPS - 250 KC, and a scale accuracy of $\pm 2\%$ was utilized for the investigation. Shielded cable for the leads is also necessary. Any good general purpose oscilloscope would be satisfactory.

V. ACOUSTIC PROBE DATA

A. Oscilloscope Data

Several oscilloscope photographs of the voltage waveforms from the crystal were taken with a Polaroid camera. Figure 12 consists of two such photos. Shown are waveforms for the mercury loop with the Plexiglas venturi in place (containing special damage specimens) at a velocity of $3\frac{1}{4}$ feet/sec. for the case of Zero cavitation and Standard cavitation. In each case the oscilloscope probe was held directly against the crystal. There is a large increase in signal as the degree of cavitation is increased from Zero to Standard. The frequency of the waveform obtained for the Standard cavitation condition is approximately 2,000 CPS, which is consistent with the rod length as previously discussed. Figure 13 indicates a sequential progression from Zero cavitation to First Mark cavitation in the mercury loop with the stainless steel venturi (standard specimen in place) at a velocity of $3\frac{1}{4}$ feet/sec. The observed frequency is much higher than that noted for the case of the Plexiglas venturi and is very difficult to estimate. In each case

100 mv./cm.

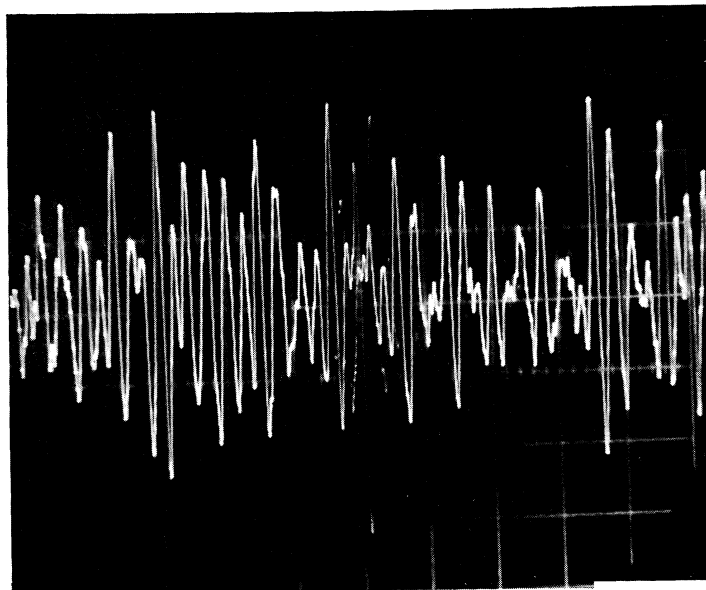


1358(a)

2 milliseconds/cm.

Figure 12(a). Zero Cavitation

100 mv./cm.



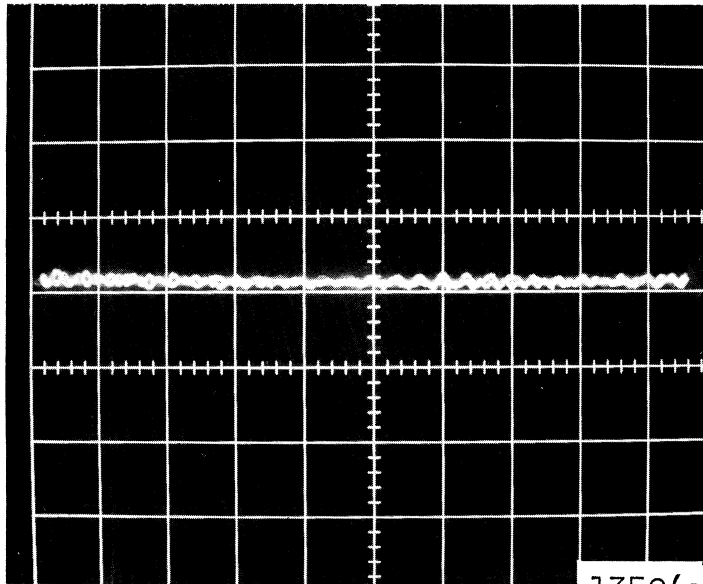
1358(b)

2 milliseconds/cm.

Figure 12(b). Standard Cavitation

Figure 12. Acoustic Probe Voltage Representation
of Cavitation Noise From Collapsing Bubbles in Mercury
Plexiglas Venturi & Velocity of 34 feet/second
Probe Touched Directly to Crystal

50 mv./cm.

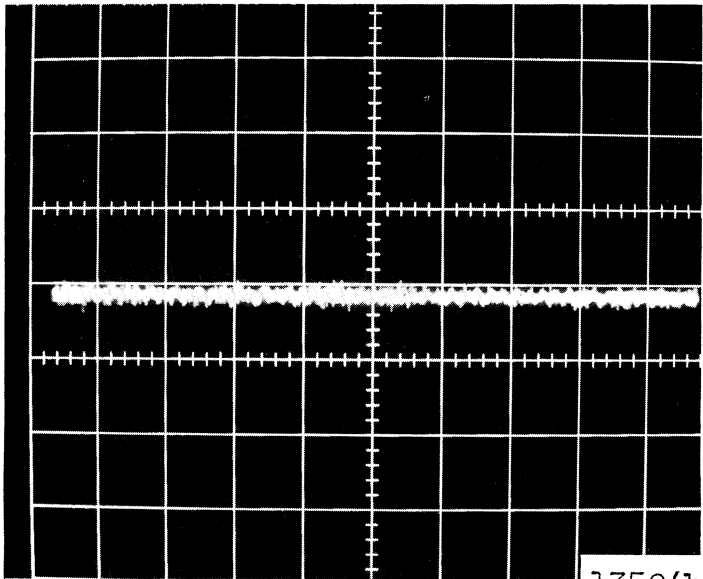


1359(a)

2 milliseconds/cm.

Figure 13(a). Zero Cavitation

50 mv./cm.



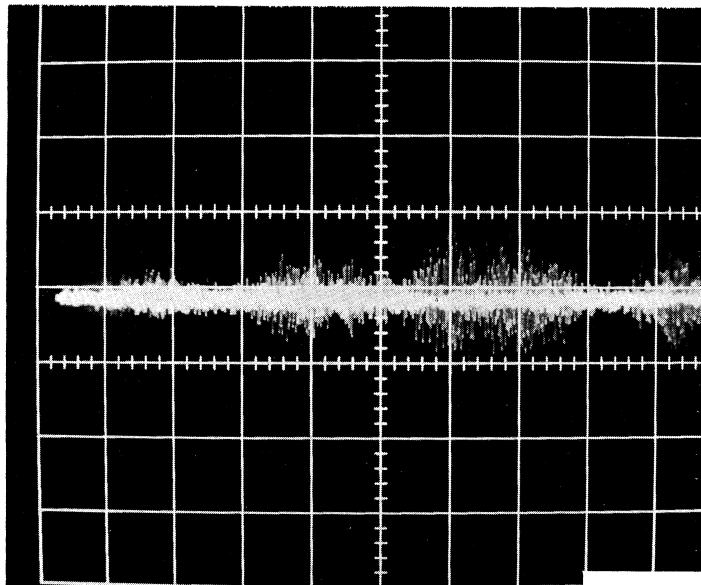
1359(b)

2 milliseconds/cm.

Figure 13(b). Visible Cavitation

Figure 13. Acoustic Probe Voltage Representation of Cavitation Noise From Collapsing Bubbles in Mercury Stainless Steel Venturi & Velocity of 34 feet/second Probe Inserted into Banana Jack

50 mv./cm.

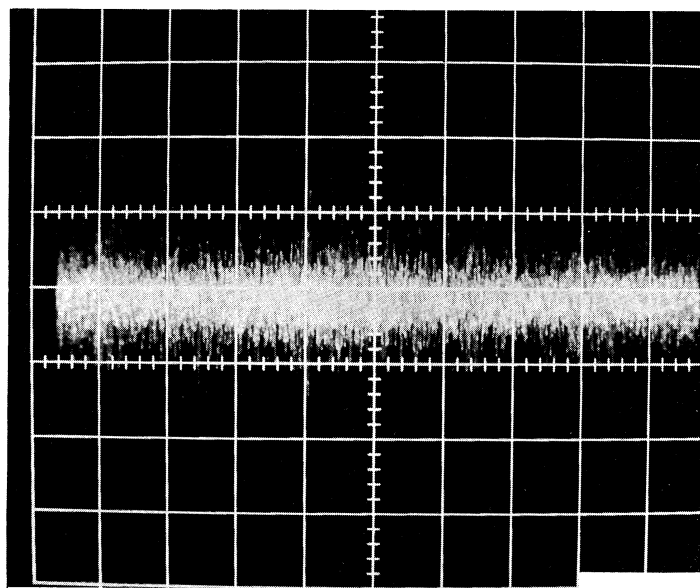


1359(c)

2 milliseconds/cm.

Figure 13(c). > Visible Cavitation

50 mv./cm.



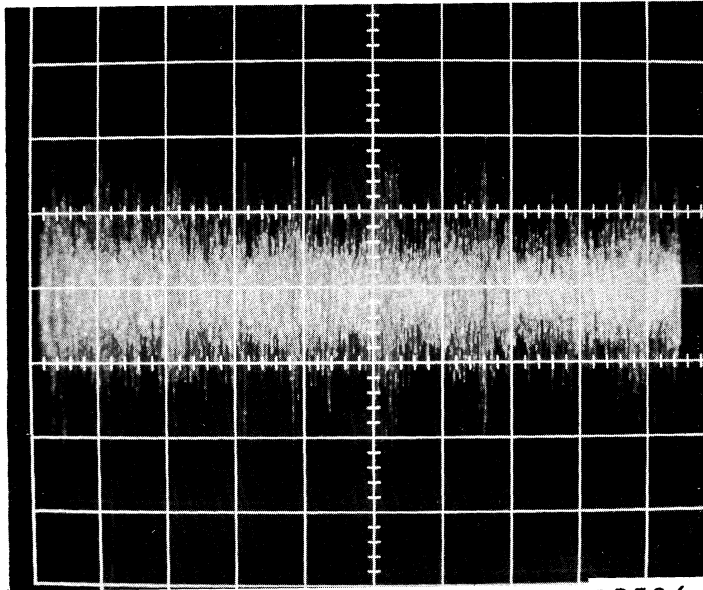
1359(d)

2 milliseconds/cm.

Figure 13(d). Nose Cavitation

Figure 13 (Continued)

50 mv./cm.

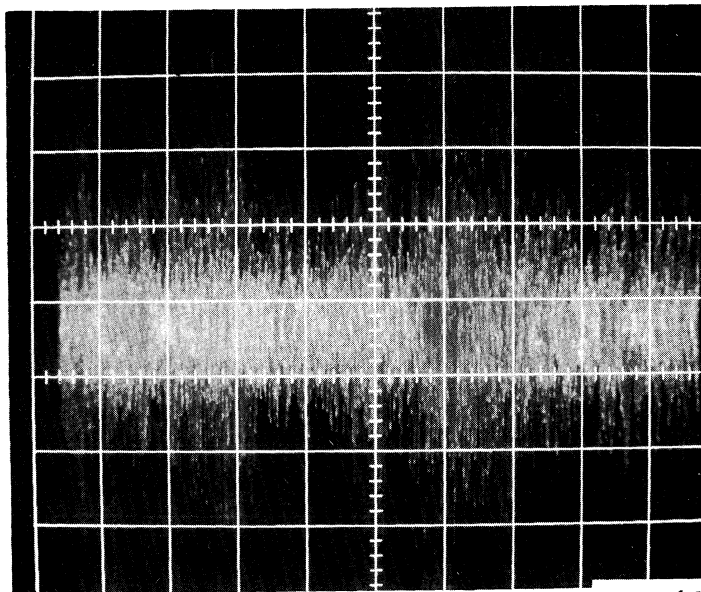


1359(e)

2 milliseconds/cm.

Figure 13(e). Standard Cavitation

50 mv./cm.



1359(f)

2 milliseconds/cm.

Figure 13(f). First Mark Cavitation

Figure 13 (Continued)

the oscilloscope probe (banana plug) was inserted into the modified banana jack which was spring-loaded against the crystal. This arrangement results in a complex path for the sound waves and is probably responsible for the higher frequencies noted in Figure 13. No photographs of voltage waveforms for the water loop investigations are available but the waveforms were noted as being similar to those obtained for the mercury loop.

B. Vacuum Tube Voltmeter Data

Readings of RMS voltage versus pressure drop across the venturi (which is related to degree of cavitation) are available for both the mercury and water loops. Figure 14 is such a plot for the mercury loop at room temperature. The stainless steel venturi was in place and contained a standard damage specimen. Investigations were made at velocities of 26 feet/sec., 34 feet/sec., and 37 feet/sec. It is clear that the RMS signal increases as the venturi Δp (extent of cavitation) increases until a plateau value is reached. Thereafter the signal is about constant. For a given cavitation condition the RMS signal is proportional to velocity to the ~ 1.7 power. Figure 15 presents data obtained at a temperature of 500 °F. and at a velocity of 34 feet/sec. A standard damage specimen was in place. The general shape of the curve is similar to that obtained in Figure 14. However, the plateau at 500 °F. appears to be about 3 mv. less than at room temperature. This might be due to the fact that the increased mercury vapor density at 500 °F. is cushioning the collapse of bubbles and hence absorbing a fraction of the sound energy. Hence, one would expect a reduced signal at the elevated temperature. Figure 16 presents additional data for the

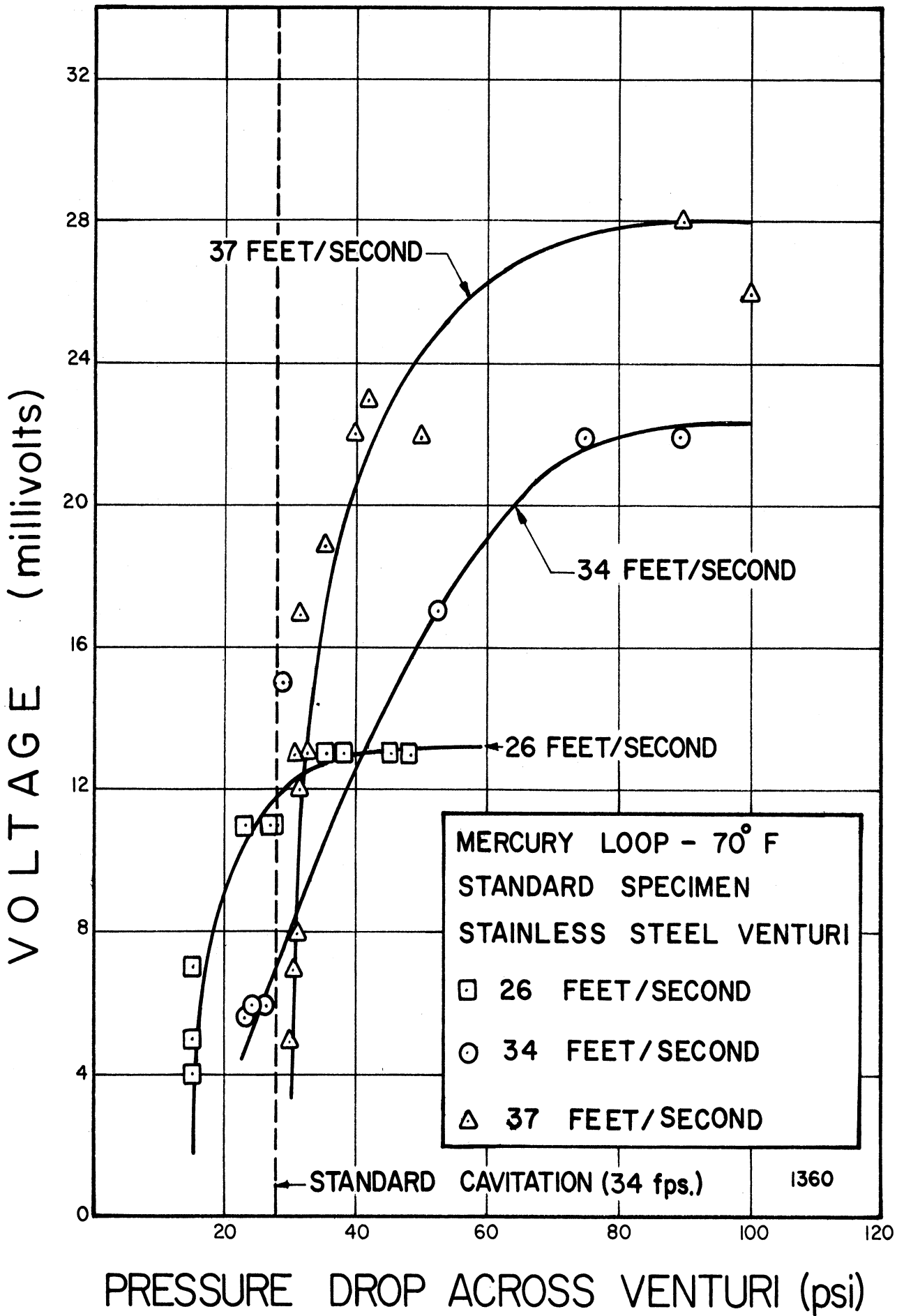


Figure 14. Effect of Cavitation Condition and Velocity on Sound Amplitude in Mercury

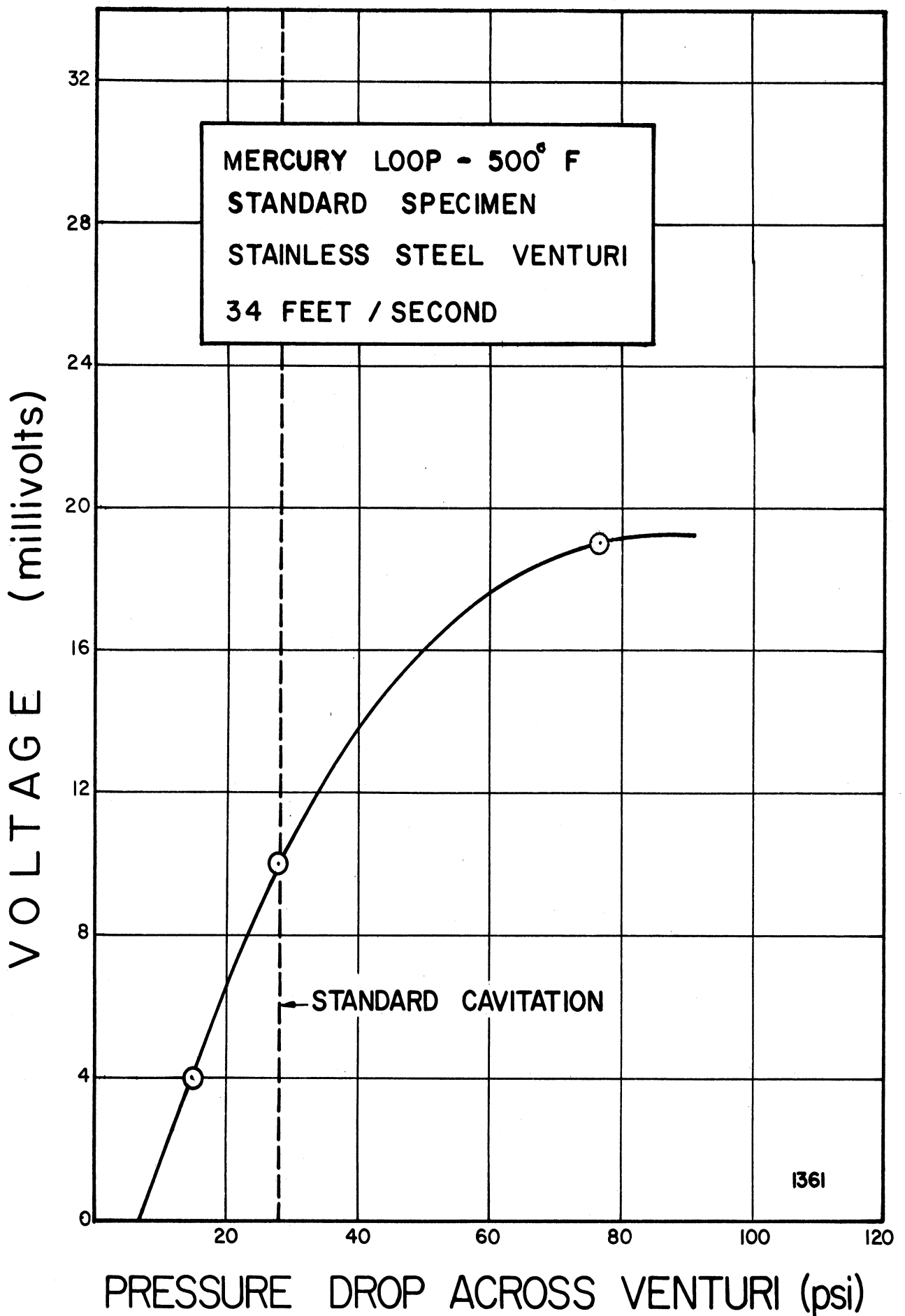


Figure 15. Effect of Cavitation Condition on Sound Amplitude in Mercury at 500°F.

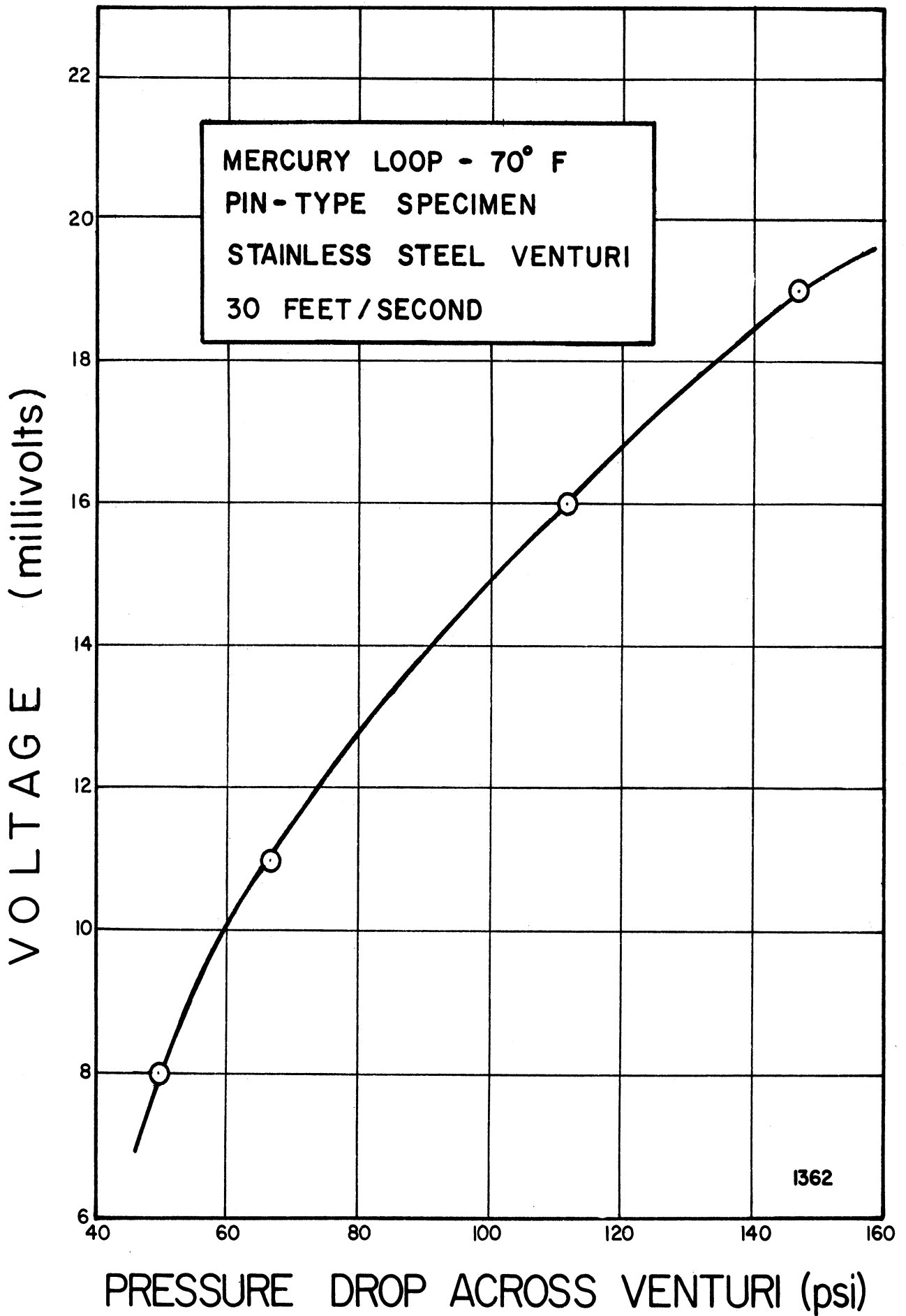


Figure 16. Effect of Cavitation Condition on Sound Amplitude in Mercury with Pin-Type Specimen

mercury loop with a pin-type specimen in the stainless steel venturi. Here the velocity is 30 feet/sec. The curve shape is similar to the others except that the plateau region is not nearly as apparent. Since the rate of damage is much greater with the pin, it might be expected that the noise level would be considerably greater. However, this is apparently not the case.

In the case of the water loop data is available at velocities of 100 feet/sec. and 200 feet/sec. with the Plexiglas venturi in place and containing standard stainless steel specimens. The temperature was ambient. Figure 17 is a plot of RMS signal versus venturi Δp at a velocity of 100 feet/sec. Figure 18 is a similar plot at a velocity of 200 feet/sec. In both cases a plateau is evident, as was the case in the mercury investigations. For a given cavitation condition the RMS signal is proportional to velocity to the ~ 1.5 power. Once again this is similar to the mercury loop results.

C. Summary and Discussion of Results

The following statements summarize the results of the acoustic probe study:

1. For mercury the cavitation signal is proportional to velocity to the ~ 1.7 power.
2. For water the cavitation signal is proportional to velocity to the ~ 1.5 power.
3. The RMS signal appears to be stronger for mercury at 34 feet/sec. than for water at 100 feet/sec. for the same cavitation condition by a factor of about 3.
4. For mercury only data with the stainless steel venturi

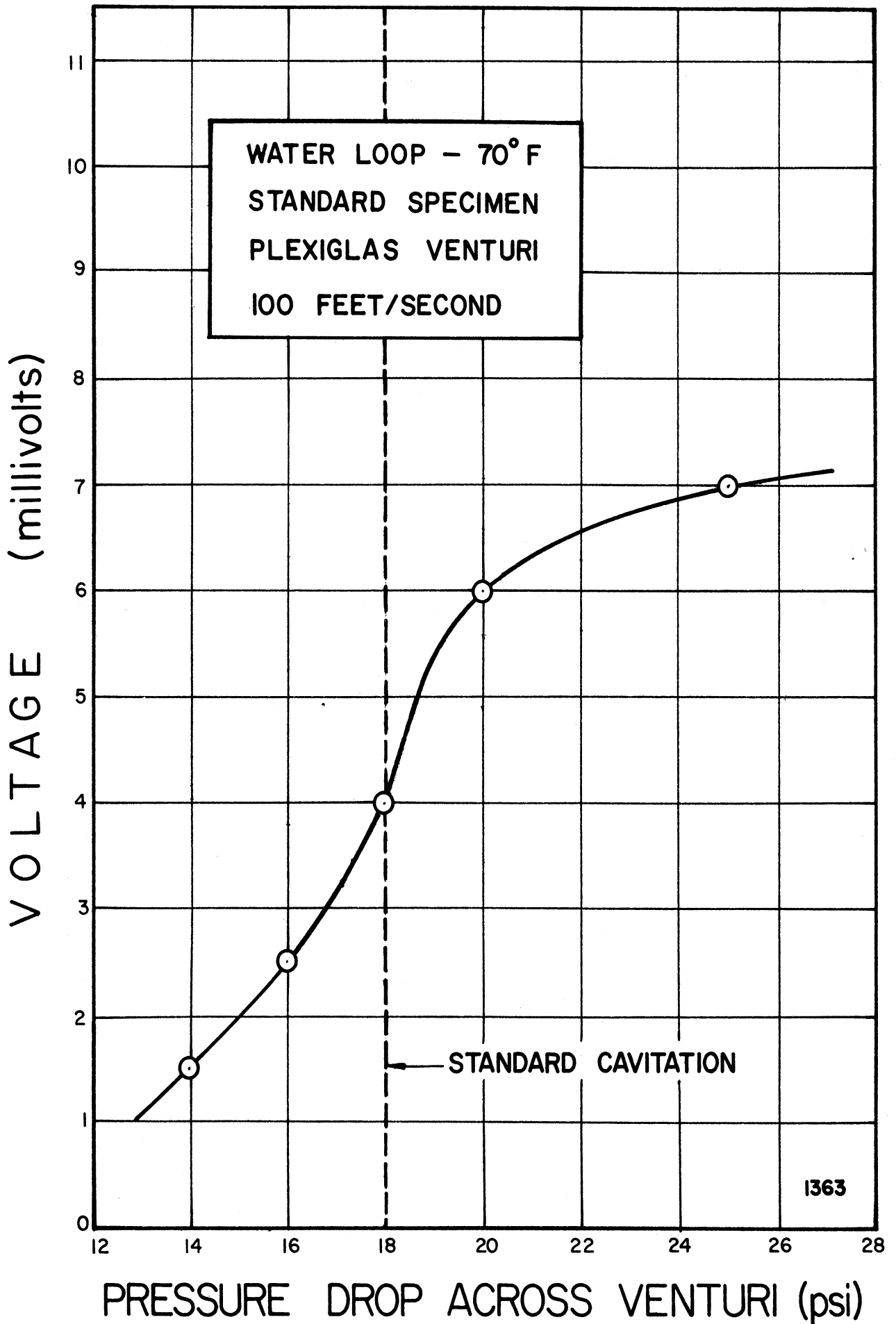


Figure 17. Effect of Cavitation Condition on Sound Amplitude in Water at 100 feet/second

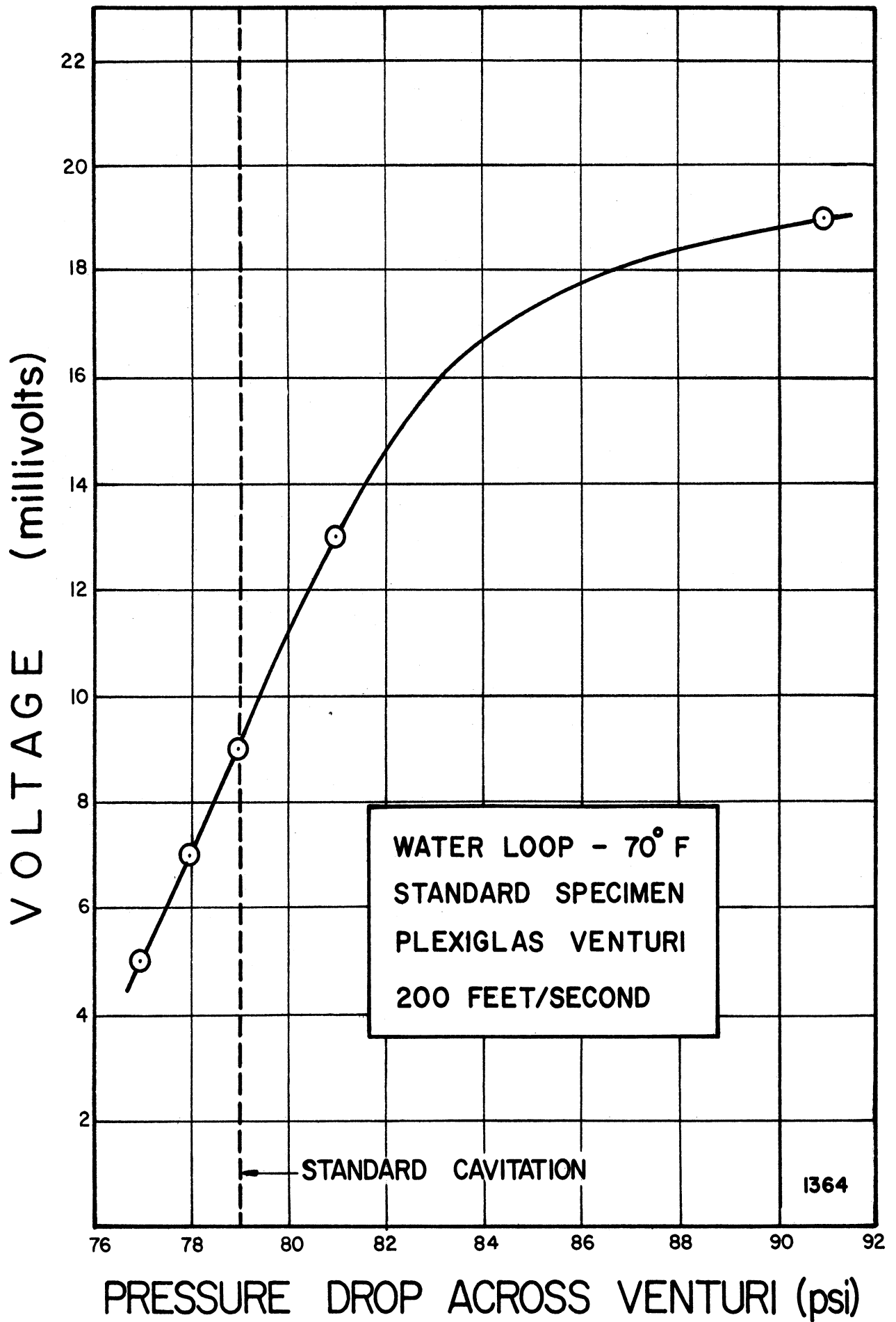


Figure 18. Effect of Cavitation Condition on Sound Amplitude in Water at 200 feet/second

are available. For water only data with the Plexiglas venturi are available. Hence no conclusions can be drawn as to the effect of venturi material on the cavitation signal.

5. For both mercury and water the signal increases as the degree of cavitation becomes more intense (venturi Δp increases). This is to be expected.

6. For mercury the signal decreases by 15% as the temperature is raised from ambient to 500 °F.

7. The frequency of the observed voltage waveforms from the crystal appears to be about 2 KC when the oscilloscope probe is held directly against the crystal. This frequency seems consistent with the 4-6 KC range of frequencies observed in the air-borne noise investigations. However, when the oscilloscope probe (banana plug) is inserted into the modified banana jack which is spring-loaded against the crystal, then the frequency of the observed voltage waveforms from the crystal is increased into the high KC range. This might be due to the complex sound path through the venturi wall, along the length of the stainless steel rod, and then through the modified banana jack to the oscilloscope probe.

8. The sonic probe technique was checked for reproducibility of results, and generally this was achieved admirably.

VI. RECOMMENDATIONS FOR AN OPTIMUM SYSTEM

The acoustic probe described in this paper appears to be satisfactory for detecting cavitation incipience, degree, and intensity by means of observing the sound pattern generated by the collapsing bubbles in the venturi test section. The sound path from

bubble to crystal is a complex one and appears to obscure needed frequency information. Perhaps threading the probe directly into the venturi would be an improvement. However, sealing problems at high temperature may then be prohibitive.

BIBLIOGRAPHY

1. Hammitt, F. G., "Cavitation Damage and Performance Research Facilities", ORA Technical Report No. O3424-12-T, Department of Nuclear Engineering, The University of Michigan, November, 1963.
2. Hammitt, F. G., "Observations on Cavitation Damage in a Flowing System", Journal of Basic Engineering, Transactions, ASME, Series D, Vol. 85, (1963) pp. 347-359.
3. Hueter, T. F., and Bolt, R. H., Sonics, John Wiley and Sons, Inc., 1955.
4. Peterman, L. A., "Cavitation Attack in Ultrasonic Equipment", Product Engineer, September, 1955.
5. Fitzpatrick, H. M., and Strasberg, M., "Hydrodynamic Sources of Sound", Naval Hydrodynamics, Publication 515, NAS-NRC, 1957.
6. Harrison, Mark, "An Experimental Study of Single Bubble Cavitation Noise", D.T.M.B. Report 815, November, 1952.
7. Mellen, R. H., "An Experimental Study of the Collapse of a Spherical Cavity in Water", Journal of the Acoustical Society of America, Vol. 28, No. 3, May, 1956.
8. Mellen, R. H., "Ultrasonic Spectrum of Cavitation Noise in Water", Journal of the Acoustical Society of America, Vol. 26, No. 3, May, 1954.
9. Den Hartog, Jacob, Mechanical Vibrations, Fourth Edition, McGraw-Hill Publishing Company, 1956.